Electronic Supplementary Information (ESI)

$CoTeO_4$ – a wide-bandgap material adopting the dirutile structure type

Matthias Weil,*[a] Prativa Pramanik,[b] Pierfrancesco Maltoni,[b] Rebecca Clulow,[c] Andreas Rydh,[d] Manfred Wildner,[e] Peter Blaha,[f] Harishchandra Singh,[g] Sergey A. Ivanov,[b] Roland Mathieu[b] and Graham King[h]

[a.] *Institute for Chemical Technologies and Analytics, Division of Structural Chemistry, TU Wien, Getreidemarkt 9/E164-05-1, A-1060 Vienna, Austria.*
[b.] *Department of Materials Science and Engineering, Uppsala University, Box 35, SE-751 03 Uppsala, Sweden.*
[c.] *Department of Chemistry, Ångström Laboratory, Uppsala University, 751 21 Uppsala, Sweden.*
[d.] *Department of Physics, Stockholm University, 106 91 Stockholm, Sweden.*
[e.] *Institut für Mineralogie und Kristallographie, Universität Wien, Josef-Holaubek-Platz 2, A-1090 Vienna, Austria.*
[f.] *Institute for Materials Chemistry, Division Theoretical Chemistry, TU Wien, Getreidemarkt 9/E165-03, A-1060 Vienna, Austria.*
[g.] *Nano and Molecular Systems Research Unit, University of Oulu, Oulu FIN-90014, Finland.*
[h.] *Canadian Light Source, 44 Innovation Blvd., Saskatoon, Saskatchewan S7N 2V3, Canada.*

A) X-ray diffraction measurements and Rietveld refinements

For phase analysis and Rietveld refinements, $CoTeO_4$ powder samples were characterized by using a Bruker D8 Advance diffractometer (solid state rapid LynxEye detector, Cu K_α radiation, Bragg–Brentano geometry, DIFFRACT plus software) in the 10°–140° 2θ range with a step size of 0.013° (counting time was 4s per step). The powder samples were ground in an agate mortar and suspended in ethanol. An Si substrate was covered with several drops of the resulting suspension, leaving randomly oriented crystallites after drying. Rietveld refinements were performed by using the FULLPROF program.[1] The peak shape of the reflections was described by a modified Thompson–Cox–Hastings pseudo-Voigt function. Background intensities were estimated by interpolating between up to 60 selected points. A NIST LaB6 660b standard was measured under the same conditions as the samples to account for the instrumental contribution to the peak broadening.

The PXRD pattern (Fig. 1) can be fully ascribed to the $CoTeO_4$ structure in the space group $P2_1/c$. For Rietveld refinement, the crystal data from the current single crystal diffraction study were taken as starting parameters. The Rietveld refinement shows good agreement between the experimental (red circular dots) and calculated data (black solid line). The refined unit-cell parameters and atomic coordinates are given in Table S1 and Table S2, respectively, and are compared to those obtained from the single-crystal study, as well as those from the previous powder studies by Patel *et al*.[2] and Isasi.[3] Within the accuracy of the method, the sample can be considered single-phase. A remarkable agreement between the current powder X-ray study and the SC study is observed, particularly concerning unit-cell parameters. Although we do not observe a drastic change in the unit-cell size compared to Patel *et al*., [2] the Co–O bond lengths and Co–O–Co bond angles determined from our laboratory data differ from the synchrotron data. [2] Such discrepancies most probably are caused by the coordinates of the O atoms and their uncertainties.

ESI Table S1. Results of Rietveld refinement based on laboratory PXRD data of polycrystalline $CoTeO_4$. Results from the current single-crystal (SC) X-ray study and from the powder synchrotron study of Patel *et al*. [2] and the powder study by Isasi [3] are added for comparison.

	Current Rietveld study	Current SC study	Powder synchrotron study	Powder study
Space group	$P2_1/c$	$P2_1/c$	$P2_1/c$	$P2_1/n$ (VO_2-like)
a /Å	5.56756(4)	5.5635(12)	5.5660(2)	6.192(3)
b /Å	4.67052(3)	4.6675(10)	4.66500(12)	4.671(3)
c /Å	5.54312(3)	5.5424(12)	5.5480(3)	5.567(2)
β /°	112.2547(4)	112.321(6)	112.323(1)	124.07(2)
V /Å^3	133.403(7)	133.14(5)	132.476(1)	133.38
R_p	4.6		11.5	9.5
R_w	5.5		13.2	9.5

ESI Table S2. Atomic coordinates and occupancies of atoms in $CoTeO_4$ as determined from the current Rietveld refinement based on laboratory PXRD data of polycrystalline $CoTeO_4$. Optimized atomic coordinates of O atoms from the current DFT calculations using PBE and PBE+U with 4.08 and 5.44 eV, respectively, are also listed. Results from the single-crystal study and from the synchrotron powder study of Patel *et al*. [2] and the powder study by Isasi [3] are added for comparison.

	X	*y*	*z*	s.o.f.	Multiplicity Wyckoff site
Current Rietveld study					
Co	0	0	0	1	2 *a*
Te	0.5	0.5	0.5	1	2 *d*
O1	0.354(1)	0.216(1)	0.172(1)	1	4 *e*
O2	0.833(1)	0.318(2)	0.130(2)	1	4 *e*
DFT Optimization					
O1 (PBE)	0.3424	0.2086	0.1608	1	4 *e*
O1 (PBE+U(4.08))	0.3480	0.2225	0.1727	1	4 *e*
O1 (PBE+U(5.44))	0.3491	0.2233	0.1737	1	4 *e*
O2 (PBE)	0.8370	0.3052	0.1437	1	4 *e*
O2 (PBE+U(4.08))	0.8263	0.3150	0.1369	1	4 *e*
O2 (PBE+U(5.44))	0.8252	0.3155	0.1363	1	4 *e*
Current SC study					
Co	0	0	0	1	2 *a*
Te	0.5	0.5	0.5	1	2 *d*
O1	0.3560(2)	0.2219(2)	0.1757(2)	1	4 *e*
O2	0.8238(2)	0.3225(2)	0.1340(2)	1	4 *e*
Synchrotron powder study[2]					
Co	0.5	0	0	1	2 *b*
Te	0	0	0.5	1	2 *c*
O1	0.623(2)	0.172(2)	0.350(2)	1	4 *e*
O2	0.140(2)	0.258(2)	0.312(2)	1	4 *e*
Powder study[3]					
Co/Te	0.258(7)	0.022(5)	0.001(9)	0.5/0.5	4 *e*
O1	0.127(3)	0.188(4)	0.222(2)	1	4 *e*
O2	0.446(8)	0.720(7)	0.357(7)	1	4 *e*

ESI Table S3. Bond lengths and angles in $CoTeO_4$ resulting from the different experimental studies and the DFT optimization.

	Current Rietveld study	Current SC study	Synchro-tron powder study [2]	Powder study [3]	DFT-optimized (PBE)	DFT-optimized (PBE+U (4.08 eV)	DFT-optimized (PBE+U (5.44 eV)
Co–O /Å	2.0867(10) 2.0956(12) 2.0205(10)	2.0619(11) 2.0812(11) 2.1163(11)	1.967 1.984 2.188	1.792(5)* 1.867(8)* 1.975(2)*	2.009 2.020 2.046	2.056 2.062 2.082	2.060 2.065 2.089
Te–O /Å	1.9779(9) 1.9184(8) 1.9663(9)	1.9625(10) 1.8619(11) 1.9667(10)	2.101 1.939 1.963	2.079(5)* 2.164(5)* 2.209(2)*	1.960 2.000 2.002	1.890 1.980 1.981	1.884, 1.977 1.978
Co–O–Co /°	123.8516(6)	121.96(5)	133	132(3) *	126.6	123.9	122.9
Te–O–Te /°	133.5171(7)	134.46(6)	137	102(3)*	129.8	132.4	132.7
Co–O–Te /°	99.2766(4) 101.1752(5) 126.2207(6) 134.5593(8)	98.53(4) 103.89(5) 125.54(5) 134.02(6)			100.6 101.0 129.1 132.4	99.1 102.9 126.7 133.9	99.0 103.0 126.4 134.1

* Co/Te on the same position with half-occupancy each. Hence, listed bond lengths and angles refer to a $[(Co,Te)O_6]$ polyhedron

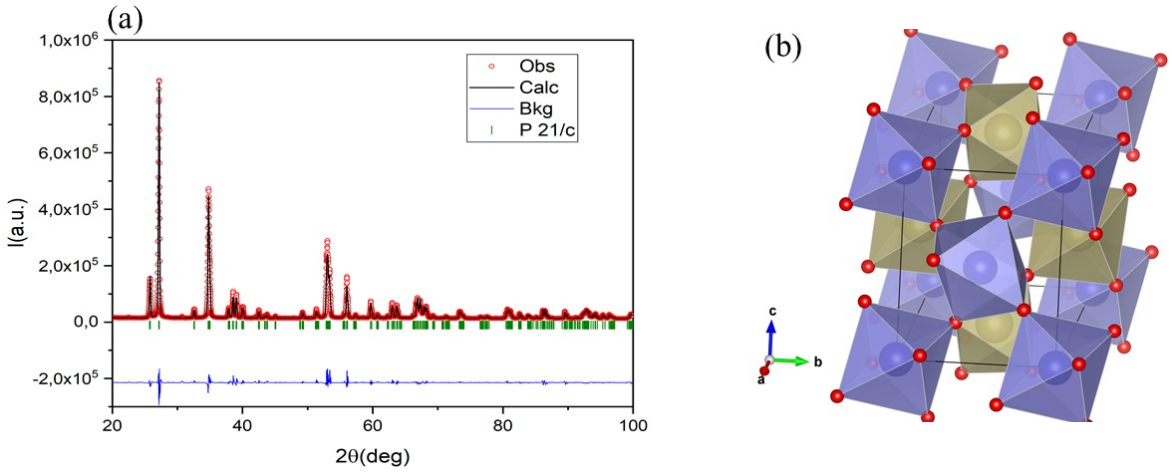

ESI Fig. S1. (a) The observed, calculated, and difference plots for the fit to the PXRD pattern of $CoTeO_4$ after the Rietveld refinement at 295 K (R_p = 4.6%, R_{wp}= 6.8% and R_{Bragg} = 4.3%). (b) Crystal structure of $CoTeO_4$ comprising corner-sharing $[CoO_6]$ (purple) and $[TeO_6]$ (yellow-grey) octahedra.

Table S4. Numerical data of regression curves for description of unit-cell parameters and

coefficients αij of the thermal expansion tensor [× 10^{-6} °C^{-1}] of $CoTeO_4$.

$a(T) = 5.56381 + 4.59157\times 10^{-5} \cdot T$; $R^2 = 0.9964$

$b(T) = 4.66648 + 5.30266\times 10^{-5} \cdot T$; $R^2 = 0.9978$

$c(T) = 5.53874 + 3.72745\times 10^{-5} \cdot T$; $R^2 = 0.9962$

$\beta(T) = 112.26 - 1.7029\times 10^{-6} \cdot T + 1.7357 \cdot T^2 - 9.3268 \times 10^{-11} \cdot T^3$; $R^2 = 0.9994$

$V(T) = 133.094 + 0.00345107 \cdot T$; $R^2 = 0.9972$

Temperature / °C	α11	α22	α33	α13
25	8.0074	11.360	6.7286	−0.6090
50	7.9819	11.357	6.7275	−0.6378
70	7.9616	11.354	6.7266	−0.6609
100	7.9311	11.350	6.7253	−0.6956
150	7.8802	11.344	6.7230	−0.75330
200	7.8293	11.338	6.7207	−0.8110
250	7.7785	11.331	6.7185	−0.8688
300	7.7275	11.325	6.7162	−0.9265
350	7.6766	11.318	6.7140	−0.9843
400	7.6256	11.312	6.7117	−1.0421
450	7.5746	11.305	6.7095	−1.0998
500	7.5236	11.299	6.7072	−1.1576
550	7.4726	11.293	6.7050	−1.2154
600	7.4215	11.286	6.7027	−1.2731
650	7.3704	11.280	6.7005	−1.3309
700	7.3192	11.274	6.6982	−1.3887
750	7.2680	11.267	6.6960	−1.4465

B) Results of energy dispersive spectroscopy (EDS) measurements

EDS measurements were carried out on two crystal aggregates of $CoTeO_4$. The oxygen content was kept constant at 66.6 at% and the Co:Te ratio determined. The results are similar for both crystals, and close to the nominal composition.

ESI Table S5: Elemental composition (at%) of $CoTeO_4$ crystals determined by energy dispersive spectroscopy (EDS). Nominal composition: Co 16.67%, Te 16.67%, O 66.67%.

Spectrum	O	Co	Te
Crystal 1			
1	66.47	17.06	16.47
2	66.65	16.69	16.65
3	66.54	16.91	16.54
4	66.5	17	16.5
5	66.6	16.8	16.6
6	66.6	16.8	16.6
7	66.5	17	16.5
8	66.64	16.73	16.64
9	66.57	16.86	16.57
10	66.58	16.84	16.58
11	66.64	16.73	16.64
Max	66.65	17.06	16.65
Min	66.47	16.69	16.47
Average	66.57	16.86	16.57
Standard deviation	0.06	0.12	0.06
Crystal 2			
1	66.86	16.28	16.86
2	66.78	16.44	16.78
3	66.77	16.47	16.77
4	66.67	16.65	16.67
5	66.74	16.52	16.74
6	66.79	16.42	16.79
7	66.75	16.5	16.75
8	66.91	16.18	16.91
9	66.65	16.7	16.65
10	66.81	16.39	16.81
11	66.69	16.62	16.69
Max	66.91	16.7	16.91
Min	66.65	16.18	16.65
Average	66.76	16.47	16.76
Standard deviation	0.08	0.16	0.08

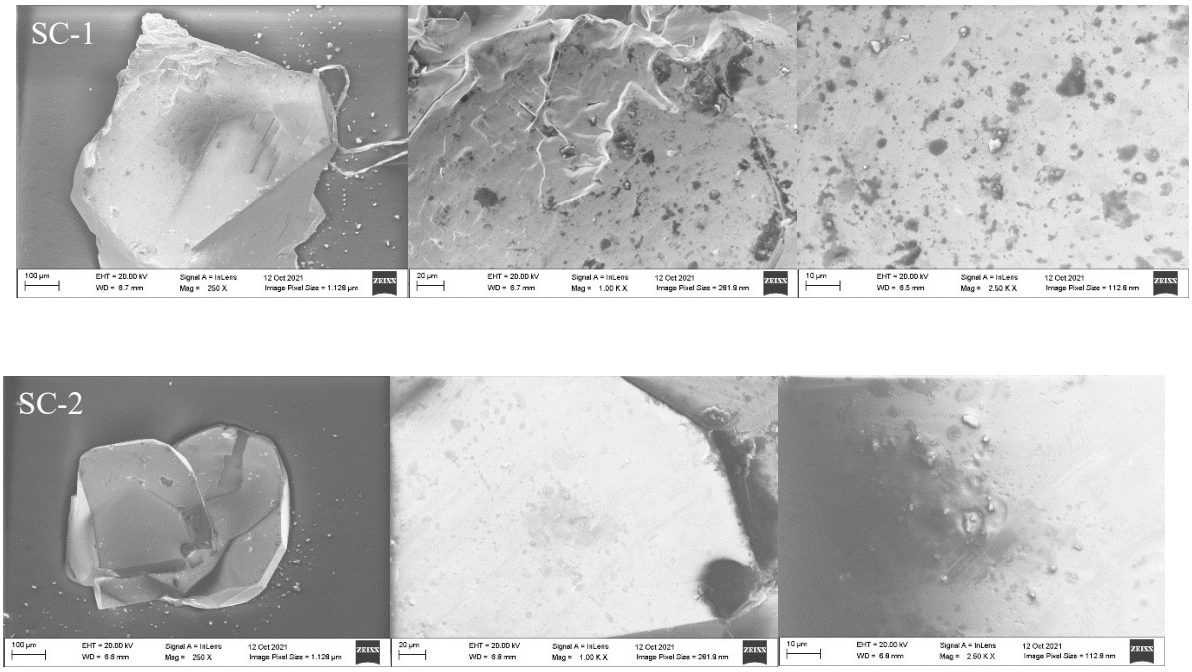

ESI Fig S2. Surface images of the two $CoTeO_4$ aggregates grown by chemical vapor transport reactions that were used for EDS measurements.

C) Results of X-ray-photoemission spectroscopy (XPS)

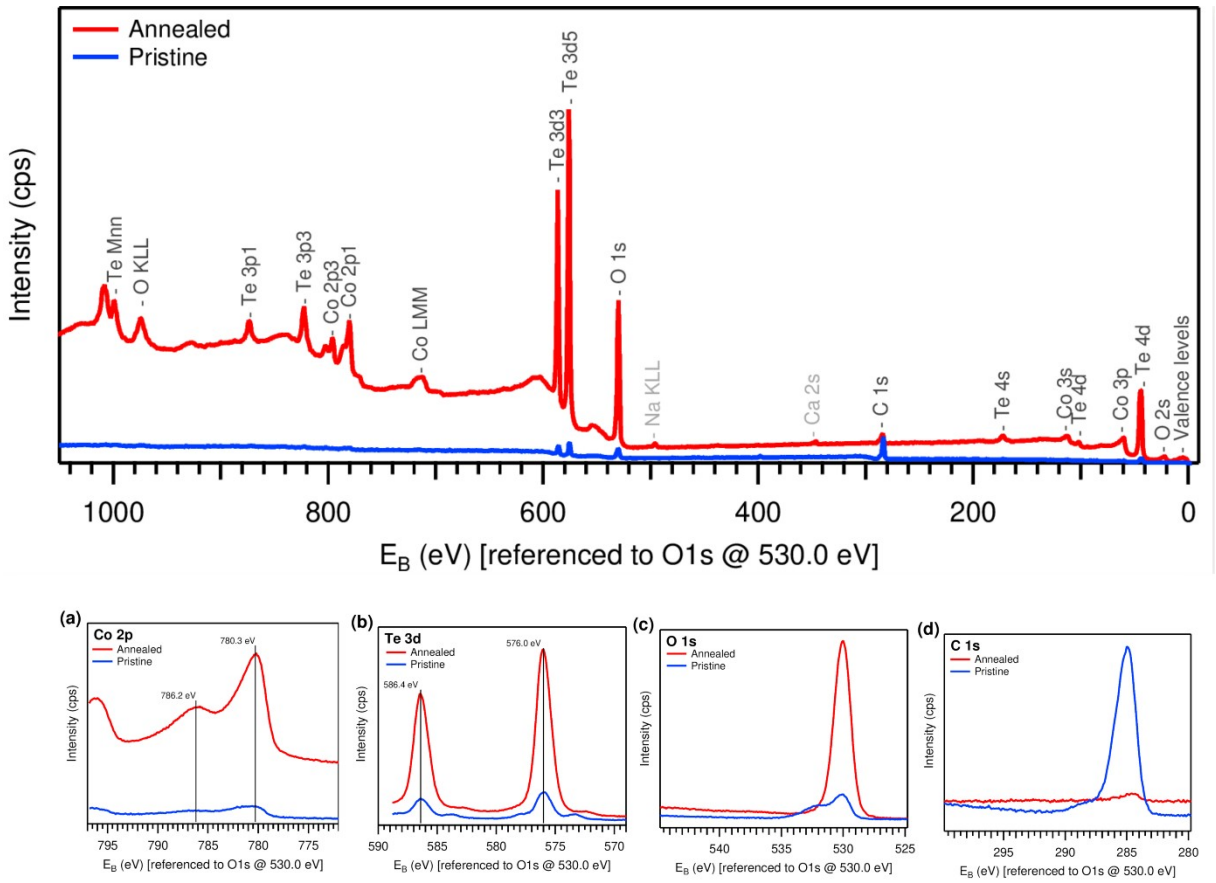

ESI Fig. S3. X-ray-photoemission spectra determined for $CoTeO_4$ crystal aggregates: Survey and spectra for (a) Co 2*p*, (b) Te 3*d*, and (c) O 1*s* and (d) C 1*s*.

D) Magnetic measurements

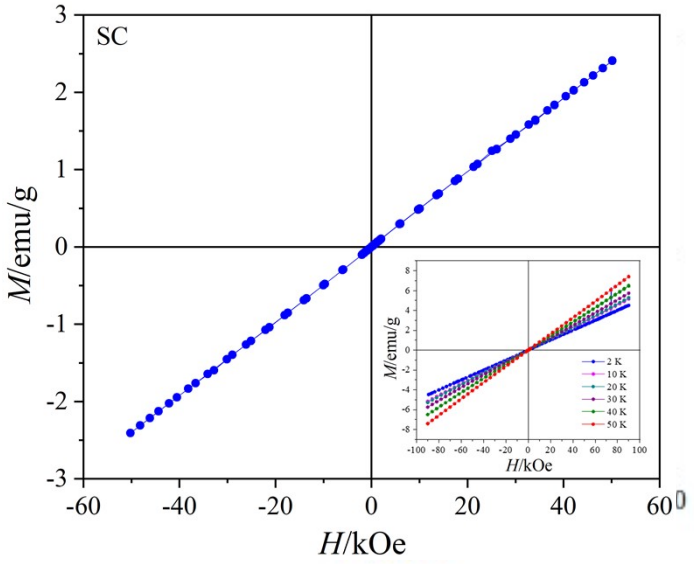

ESI Fig. S4. *M* vs. *H* at 2 K. Inset shows *M* vs *H* at various temperatures.

E) Temperature-dependence of the dielectric properties

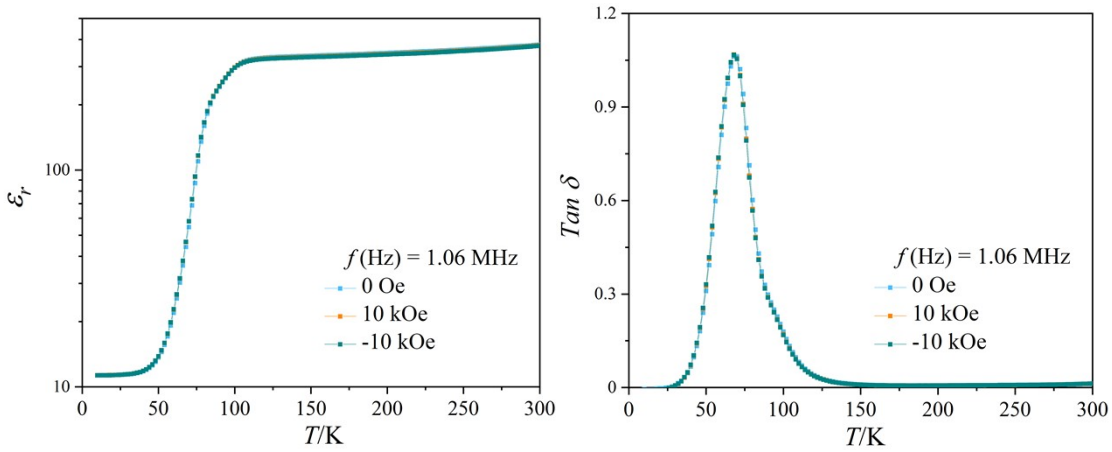

ESI Fig. S5. ε_r vs. *T* plot (left) and Tanδ vs. *T* plot (right) of $CoTeO_4$ crystals at *f* = 1.06 MHz for 0 and ± 10 kOe applied magnetic field.

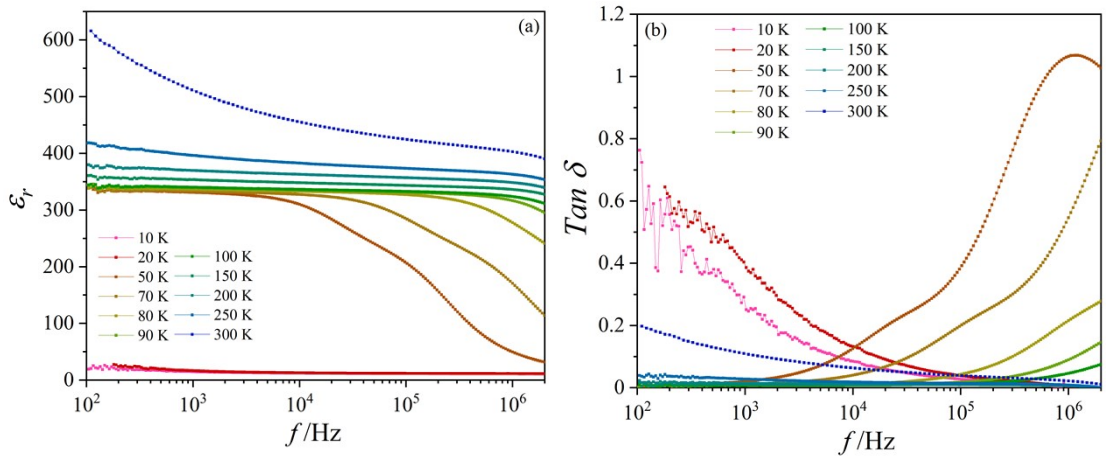
(a)
ε_r
600
500
400
300
200
100
0
10^2
10^3
10^4
10^5
10^6
f/Hz
10 K
20 K
50 K
70 K
80 K
90 K
100 K
150 K
200 K
250 K
300 K
(b)
Tan δ
1.2
1
0.8
0.6
0.4
0.2
0
f/Hz

ESI Fig S6. (a) ε_r vs *f* plot and (b) Tanδ vs *f* plot of $CoTeO_4$ crystals at different temperatures.

References

1 J. Rodríguez-Carvajal, Recent Advances in Magnetic Structure Determination by Neutron Powder Diffraction. *Physica B*, 1993, **192**, 55–69.

2 A. K. Patel, M. R. Panda, E. Rani, H. Singh, S. S. Samatham, A. Nagendra, S. N. Jha, D. Bhattacharyya, K. G. Suresh and S. Mitra, Unique Structure-Induced Magnetic and Electrochemical Activity in Nanostructured Transition Metal Tellurates $Co_{1-x}Ni_xTeO_4$ (x = 0, 0.5, and 1), *ACS Appl. Energy Mater.*, 2020, **3**, 9436–9448.

3 J. Isasi, New $MM'O_4$ Oxides Derived from the Rutile Type: Synthesis, Structure and Study of Magnetic and Electronic Properties, *J Alloys Compd*., 2001, **322**, 89–96.